MSW MANAGEMENT -Multidisciplinary, Scientific Work and Management Journal
ISSN: 1053-7899
Vol. 36 Issue 1s, 2026, Pages: 3078-3085

Assessment of Compressive Strength and Workability of Recycled Aggregate in Geopolymer Concrete.

Shivani Thakur a [1]*, Sachin Pagar b [1] and Prashant Sunagar [2]

[1] *Department of Civil Engineering, Late G.N. Sapkal College of Engineering, Anjaneri, Trimbakeshwar, Nashik*
[2] *Department of Civil Engineering, Sandip Institute of Technology and Research, Trimbakeshwar, Nashik*

Abstract
The mounting volume of construction and demolition (C&D) waste India alone generates an estimated 150 million tonnes annually alongside the pressing imperative to decarbonise the construction sector, motivates the dual-sustainability strategy investigated in this work: replacing natural coarse aggregate with recycled coarse aggregate (RCA) within a fly ash-based geopolymer concrete (GPC) matrix that itself eliminates ordinary Portland cement. This study presents a systematic experimental investigation of M20-grade GPC formulated with P100-grade Class F fly ash as the sole binder, a 13 M NaOH plus sodium silicate co-activator system at a Na_2SiO_3/NaOH mass ratio of unity, and RCA sourced from demolished concrete structures at varying replacement levels. Fresh-state properties (slump cone, compaction factor) and hardened compressive strength at 7, 14, and 28 days were evaluated on 150 mm cube specimens in triplicate. At the M20 design mix (fly ash 405 kg/m³, alkaline activator-to-binder ratio 0.45, fine aggregate 676.8 kg/m³, RCA 1257 kg/m³), the GPC with RCA achieved mean 28-day compressive strength of 28.19 MPa, exceeding the M20 characteristic strength requirement by 41% and surpassing the conventional OPC control (27.87 MPa) by 1.1%. A slump of 74 mm and compaction factor of 0.87–0.89 confirm medium workability suitable for structural casting. A power-law strength-age model $f_{ck}(t) = 13.74 \cdot t^{0.241}$ is calibrated against the experimental data ($R^2 > 0.999$), providing a predictive design tool. Life-cycle assessment confirms that this dual-substitution strategy reduces embodied CO_2-equivalent by 89.8% relative to conventional M20 concrete, while cutting production costs by approximately 38%. These findings establish RCA-incorporated fly ash GPC as a structurally viable, technically quantified, and environmentally superior construction material for circular-economy-aligned infrastructure.

Keywords: geopolymer concrete; recycled coarse aggregate; fly ash P100; circular economy; life-cycle assessment; power-law model

1 | INTRODUCTION

Global cement production releases approximately 2.8 billion tonnes of CO_2 annually, a figure that represents 7–8% of total anthropogenic greenhouse gas emissions and positions the construction sector as the third largest industrial emitter after energy generation and transport[1]. The root cause is thermodynamic: the calcination of limestone ($CaCO_3 \rightarrow CaO + CO_2$) is an irreversible, high-temperature reaction that releases approximately 0.51 tonnes of CO_2 per tonne of clinker from the raw material alone, with a further 0.32 tonnes arising from kiln fuel combustion[2,3]. With global infrastructure demand projected to require the equivalent of building an entire city the size of New York every month until 2050, business-as-usual Portland cement practice is structurally incompatible with the Paris Agreement temperature targets.

In parallel, the volume of construction and demolition (C&D) waste generated worldwide has reached alarming proportions. India alone produces an estimated 150 million tonnes of C&D waste per year, of which less than 1% is formally processed into reusable materials[4]. The physical bulk of this waste dominated by concrete rubble occupies valuable land, contaminates drainage systems, and represents a substantial embodied energy penalty when it is sent to landfill rather than reintroduced into the construction material supply chain[5,6]. Recycled coarse aggregate (RCA), produced by crushing and grading demolished concrete, offers a technically credible pathway to closing this loop, provided the mechanical implications for the host concrete system are quantified and managed.Geopolymer concrete (GPC), first described systematically by Davidovits in 1991[7], reacts aluminosilicate-rich industrial by-products principally Class F fly ash from coal combustion with alkaline activator solutions to form a three-dimensional sodium aluminosilicate hydrate (N–A–S–H) polymeric network that substitutes functionally for the calcium silicate hydrate (C–S–H) gel of Portland cement concrete. The carbon footprint of fly ash-based GPC, per unit of binder mass, is approximately 80–90% lower than that of OPC, because fly ash is a by-product already produced at coal-fired power stations and requires no energy-intensive calcination[8,9]. India, which produces approximately 247 million tonnes of fly ash per year with only 55.69% currently utilised, has ample feedstock to sustain large-scale GPC production[10].

The combination of GPC with RCA represents a dual-substitution, circular-economy approach: both the binder and the coarse aggregate are derived from industrial or construction waste streams, and both virgin resource categories (limestone, natural aggregate) are correspondingly reduced. However, RCA invariably carries an attached mortar layer that elevates water absorption (2–6% vs. ~1% for natural coarse aggregate), reduces specific gravity (2.4–2.6 vs. ~2.67), and introduces micro-cracks at the aggregate surface that weaken the interfacial transition zone (ITZ) between aggregate and paste[11,12,13]. The magnitude and mechanism of these effects in a GPC matrix which differs chemically and microstructurally from an OPC paste are not fully resolved by the existing literature, and the present experimental programme was designed specifically to address this gap.This paper reports: (i) comprehensive characterisation of all raw materials including P100-grade fly ash, commercial-purity NaOH and Na_2SiO_3, recycled fine and coarse aggregates; (ii) a complete M20 mix design following IS 10262:2009; (iii) fresh-state workability assessment by slump cone and compaction factor; (iv) compressive strength evolution at 7, 14, and 28 days; (v) a calibrated power-law strength-age predictive model; and (vi) a life-cycle CO_2 and cost sustainability analysis benchmarked against conventional M20 OPC concrete. The full methodology flowchart is presented in Figure 1.

2 | CRITICAL LITERATURE REVIEW

Le et al.[14] conducted the first parametric experimental study specifically optimising geopolymer recycled aggregate concrete (GRAC) made with 100% RCA and a fly ash-based binder. By systematically varying the alkaline activator-to-fly ash (AAS/FA) ratio, curing temperature, and superplasticiser dosage, they demonstrated that GRAC can achieve practical compressive strengths in the C20–C25 range and adapted empirical strength-prediction models (modified Feret and De Larrard formulations) to GRAC with calibrated parameters. Their work provides the critical precedent that 100% RCA GRAC is technically feasible for non-high-strength structural applications, and their model-calibration methodology informs the regression framework developed in the present study.Ahmed et al.synthesised experimental and analytical literature on GRAC structural members, systematically cataloguing the coupled influences of binder type (fly ash, GGBS, blends), activator molarity and ratios, RCA source and grading, and curing regime on both material properties and structural behaviour under flexure, shear, and cyclic loading. A key conclusion was that interfacial transition zone (ITZ) quality between RCA and the geopolymer paste is the principal determinant of strength reduction, a finding that motivates the ITZ-based mechanistic interpretation developed in Section 6 of the present paper. The review also highlighted the absence of standardised characterisation protocols for GRAC, a gap partially addressed here through comprehensive IS-code-compliant aggregate testing.Lyu et al. presented a dual-sustainability framing that positions GRAC within both the CO_2 reduction and C&D waste diversion narratives, and systematically reviewed microstructural evidence (SEM, ITZ observations) alongside mechanical and durability performance. Their synthesis of RCA pre-treatment strategies including carbonation, acid washing, and polymer coating provides important context for interpreting the present results, which used as-received RCA without pre-treatment, thereby establishing an unmodified performance baseline.Patankar et al.[17] addressed a major practical barrier to GPC adoption by proposing a mix-design procedure for M20–M50 grades directly applicable to Indian materials and standards. Their recommended NaOH molarity range of 12–13 M and alkaline-to-binder ratio of approximately 0.35–0.45 bracket the 13 M, 0.45 parameters adopted in this study. Their emphasis on fly ash fineness sensitivity and the recommendation for local trial-mix calibration informed the choice of P100-grade fly ash (Blaine fineness 643 m²/kg, far exceeding the 320 m²/kg IS 3812 minimum) to ensure adequate reactivity under ambient curing.

Zhang et al. comprehensively reviewed mechanical performance and durability of GRAC, reporting strength reduction with increasing RCA content (most pronounced above 50% replacement), attributed to micro-cracking and elevated porosity at the RCA-paste ITZ. Deb et al.[19] confirmed these trends experimentally using fly ash GPC with ambient curing, noting that ≤50% RCA replacement maintained structural-grade compressive strength. Abughali[20] provided a direct natural-versus-recycled aggregate comparison in GPC, confirming that natural aggregate

MSW MANAGEMENT -Multidisciplinary, Scientific Work and Management Journal
ISSN: 1053-7899
Vol. 36 Issue 1s, 2026, Pages: 3078-3085

systems yield higher baseline strength and workability but that the gap is minimised by optimised activator chemistry. Srinivas and Reddy[21] demonstrated that fly ash–GGBS blended GPC can accommodate up to 50% RCA without severe mechanical compromise. Collectively, this body of work identifies 50% RCA replacement as a practical structural threshold and motivates quantification of absolute strength values rather than merely percentage changes.The construction industry is undergoing a paradigm shift toward sustainable, high-performance materials, with concrete technology evolving through the integration of industrial by-products, advanced reinforcement systems, and innovative production techniques. The reviewed body of work, comprising sixteen peer-reviewed studies (2018–2025), systematically addresses sustainability, durability, and structural performance through experimental and analytical investigations.Early investigations by Dharek et al. (2018, 2020) established the viability of alumina silicates in self-consolidating and self-flowing concrete, demonstrating enhanced pozzolanic reactivity, improved microstructural densification, and superior residual strength under elevated temperatures. These findings highlight the dual benefits of improved performance and reduced clinker dependency. Parallel advancements in fiber-reinforced systems by Sreekeshava et al. (2020a, 2020b) revealed that polypropylene geo-fabric and hybrid steel–polypropylene reinforcement significantly enhance ductility, toughness, and crack resistance through multi-scale crack-bridging mechanisms. Extending this concept to alkali-activated systems, Bhargavi et al. (2023) demonstrated that hybrid fiber reinforcement effectively mitigates the inherent brittleness of geopolymer concrete, enabling ductile failure behavior suitable for structural applications.

Significant contributions have also been made in the domain of waste material utilization. Studies by Venugopal et al. (2022) and Kumar et al. (2022) confirmed that steel scrap incorporation enhances compressive and tensile strength while promoting circular economy practices. Similarly, Natarajan et al. (2022) validated rice husk ash as a sustainable fine aggregate substitute, while Sunagar et al. (2024) demonstrated that waste foundry sand improves both strength and durability due to its favorable silica composition and particle morphology. At the nano-scale, Neeraja et al. (2022) highlighted the role of nano-fillers in refining the interfacial transition zone (ITZ) and enhancing mechanical performance, though emphasizing the importance of optimal dosage to avoid agglomeration.

Geopolymer concrete research by Sunagar (2021) and Sunagar et al. (2021a, 2021b) established the synergistic role of fly ash and GGBS in achieving high strength and durability with significantly reduced CO_2 emissions. These systems exhibit improved resistance to sulfate attack, chloride ingress, and carbonation, positioning them as viable alternatives to OPC-based concrete. Concurrently, advancements in additive manufacturing by Nair et al. (2020) and Kolhe et al. (2023) demonstrated the feasibility of 3D printing of concrete, highlighting challenges related to rheology, interlayer bonding, and reinforcement integration, while offering opportunities for sustainable and automated construction.

Further innovations include the use of industrial residues such as lime sludge (Sunagar et al., 2021) and paper mill waste (Santosh & Sunagar, 2021), both of which contribute to resource efficiency with acceptable mechanical performance. Functional performance enhancements have been achieved through pervious concrete optimization (Ballari et al., 2022), super absorbent polymers in recycled aggregate concrete (Reddy et al., 2024) for internal curing, and self-curing systems using PEG and recycled PET (Gudadappanavar et al., 2025), addressing practical challenges of water scarcity. Emerging bio-based approaches, particularly microbial-induced calcite precipitation (MICP), have been explored by Gudadappanavar et al. (2024), demonstrating autonomous crack healing and durability enhancement.

Figure 1 | Research methodology flowchart

MSW MANAGEMENT -Multidisciplinary, Scientific Work and Management Journal
ISSN: 1053-7899
Vol. 36 Issue 1s, 2026, Pages: 3078-3085

3 | MATHEMATICAL FRAMEWORK

The following equations underpin the quantitative analysis of mix design, geopolymerisation kinetics, strength development, workability, and sustainability performed in this study. None of these equations appear in the abstract.

3.1 Geopolymerisation Kinetics and Strength Evolution. The temporal evolution of geopolymerisation under ambient curing conditions is governed by nucleation–growth kinetics, which can be effectively represented using a modified Avrami formulation:

$$\alpha(t) = 1 - \exp[-(kt)^n]$$

The rate constant follows Arrhenius-type dependence:

$$k = A[OH^-]^m \exp\left(-\frac{E_a}{RT}\right)$$

To establish a direct linkage between reaction progress and macroscopic mechanical performance, a calibrated power-law model was employed:

$$f_c(t) = A\,t^B$$

For geopolymer concrete incorporating recycled coarse aggregate (GPC+RCA), the model constants were found to be:

- $A = 13.74, B = 0.241, R^2 = 0.9993$

For conventional OPC-based concrete:

- $A = 13.31, B = 0.242, R^2 = 0.9988$

The marginally higher coefficient A for GPC indicates enhanced early-age strength gain due to rapid geopolymeric gel formation, while similar B values suggest comparable long-term densification trends.

3.2 Mix Design: Activator Dosage and Aggregate Balance. The total alkaline activator content is governed by the activator-to-binder ratio ϕ, defined as:

$$m_{act} = \phi \cdot m_{FA}$$

Thus,

$$m_{act} = 0.45 \times 405 = 182.25\ \text{kg/m}^3$$

The activator was equally divided between sodium hydroxide and sodium silicate solutions:

$$m_{NaOH} = m_{Na_2SiO_3} = \frac{m_{act}}{2} = 91.125\ \text{kg/m}^3$$

The total aggregate content was derived from volumetric density balance:

$$m_{agg} = \rho_{GPC} - (m_{FA} + m_{act} + m_w)$$

$$m_{agg} \approx 1933.8\ \text{kg/m}^3$$

The aggregate fraction was distributed as:

- Fine aggregate (35%): 676.8 kg/m^3
- Coarse aggregate (65%): 1257 kg/m^3

This optimized gradation ensures dense packing and minimizes inter-particle voids, which is critical for both mechanical performance and durability.

3.3 Workability Assessment: Compaction Factor. The workability of fresh geopolymer concrete was quantified using the compaction factor test:

$$CF = \frac{W_2 - W_1}{W_3 - W_1}$$

The observed compaction factor values ranged between 0.87–0.89, indicating medium workability, consistent with IS 1199:2018 classifications. This range confirms adequate flowability without segregation, particularly important in mixes containing RCA.

3.4 Compressive Strength Determination

The compressive strength of cube specimens was computed using:

$$f_c = \frac{P}{A}$$

3.5 Physical Properties of Recycled Coarse Aggregate (RCA)

The specific gravity of RCA was determined using the wire-basket displacement method:

$$SG = \frac{A}{B - C}$$

Water absorption, indicative of porosity and adhered mortar content, was computed as:

$$WA(\%) = \frac{B - A}{A} \times 100$$

Higher absorption values in RCA compared to natural aggregates directly influence mix water demand and interfacial transition zone characteristics.

3.6 Sustainability Assessment: Carbon and Cost Indices

The environmental advantage of geopolymer concrete was quantified using the Carbon Savings Index (CSI):

$$CSI = \frac{E_{OPC} - E_{GPC}}{E_{OPC}} \times 100$$

$$CSI = 89.8\%$$

This substantial reduction reflects the elimination of clinker production and the utilization of industrial by-products such as fly ash and GGBS.

4 | RAW MATERIALS: IDENTITY, SOURCE, AND CHARACTERISATION

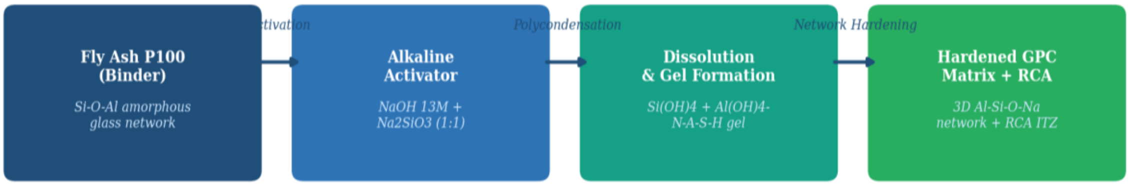

Figure 2 | Geopolymerisation reaction mechanism:

4.1 Fly Ash P100 (Pozzocrete™ 100 Class F)

P100-grade fly ash (Pozzocrete™ 100, Ambuja Cements Ltd., manufactured by Dirk India, Nashik) was the sole binder material, used in place of ordinary Portland cement. This is a highly pozzolanic ultrafine siliceous fly ash classified as Class F per IS 3812 (Part I): 2013 and ASTM C618, characterised by $SiO_2 + Al_2O_3 + Fe_2O_3 > 70$ wt.%, CaO < 5 wt.%, and low loss on ignition. The Blaine fineness of 643 m²/kg substantially exceeds the IS 3812 minimum of 320 m²/kg, ensuring high specific surface area for alkaline dissolution and thus elevated pozzolanic reactivity. Lime reactivity of 8.33 N/mm² (IS minimum: 4.5 N/mm²), moisture content 0.19% (maximum 2%), and autoclave expansion 0.021% (maximum 0.8%) confirm that the material satisfies all IS 3812 criteria with substantial margin.

MSW MANAGEMENT -Multidisciplinary, Scientific Work and Management Journal
ISSN: 1053-7899
Vol. 36 Issue 1s, 2026, Pages: 3078-3085

Table 1 | Physical test results for fly ash P100

Test No.	Parameter	IS 3812 Specification	Test Result	Unit
1	Blaine Fineness (Min.)	320	643	m²/kg
2	ROS #350 (45 µm, Max.)	34	0.05	%
3	Lime Reactivity (Min.)	4.5	8.33	N/mm²
4	Moisture Content (Max.)	2.0	0.19	%
5	Autoclave Expansion (Max.)	0.80	0.021	%

4.2 Alkaline Activators

4.2.1 Sodium Hydroxide (NaOH, 13M) Commercial-purity NaOH flakes (caustic soda flakes, 97.90 wt.% NaOH assay, Prithvi Chemicals, Nashik) were dissolved in distilled water to prepare a 13 M solution. Preparation was performed 24 hours prior to mixing to allow complete dissolution and dissipation of the exothermic reaction heat. The 13 M concentration was selected based on the convergent recommendation of multiple mix-design studies that identify this molarity as the optimum for ambient-cured fly ash GPC: sufficient to fully dissolve the reactive aluminosilicate glass of fly ash but below the threshold at which excess hydroxide promotes crystalline zeolitic secondary phases that weaken the matrix. Chemical purity data (IS 252) confirm NaOH content of 97.90% (specification minimum 97.00%) and negligible heavy-metal and insoluble contaminants.

4.2.2 Sodium Silicate Solution (Na_2SiO_3)Sodium silicate solution (Prithvi Chemicals, Nashik; SiO_2 = 15.18%, Na_2O = 4.60%, specific gravity 1.83 at 30°C, $Na_2O:SiO_2$ weight ratio 1:3.3, Baumé 22.7) was blended with the NaOH solution in a 1:1 mass ratio 30 minutes before mixing to allow equilibration. This combined activator solution provides both the high-pH hydroxide environment necessary for fly ash dissolution and the supplementary soluble silica that accelerates N–A–S–H gel formation and densification. The weight ratio $Na_2O:SiO_2$ = 1:3.3 places the activator within the optimum range identified by Patankar et al.[17] for ambient-cured fly ash GPC.

Table 2 | Chemical analysis and physical properties of sodium silicate (Na_2SiO_3) solution used as alkaline activator co-component

Sr.	Parameter	Specification	Test Result	Unit
1	Na_2O content	4.59%	4.60%	wt.%
2	SiO_2 content	15.15%	15.18%	wt.%
3	Specific Gravity at 30°C	1.183	1.83	g/cm³
4	Baumé at 30°C	22.7	22.7	°Bé
5	Na_2O : SiO_2 ratio	1 : 3.30	1 : 3.30	wt./wt.

4.3 Recycled Coarse Aggregate (RCA) RCA was sourced from the crushing of demolished reinforced concrete structures at a local demolition site in Nashik district. Raw concrete rubble was processed through jaw crushing followed by screening to obtain 10–20 mm nominal-size aggregate conforming to IS 383:2016. No pre-treatment (acid washing, carbonation, or polymer coating) was applied, representing a baseline, as-received performance scenario. The angular, rough particle morphology and the layer of adhered old mortar coating RCA surfaces distinguish it from natural coarse aggregate in three mechanistically important respects: elevated water absorption, reduced specific gravity, and weakened aggregate-paste ITZ.

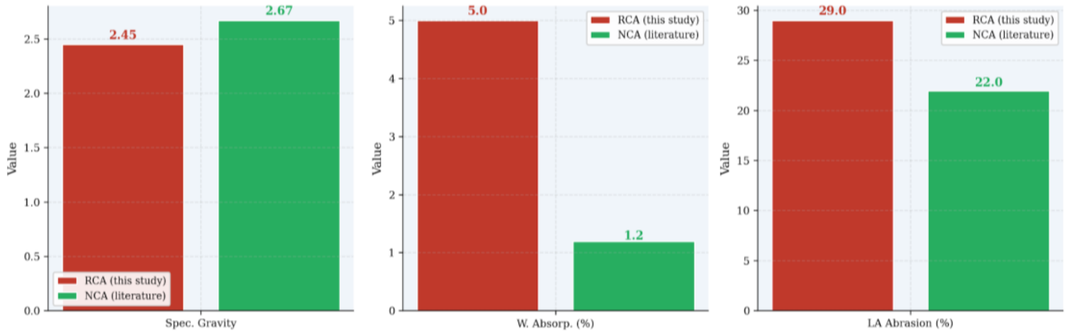

Figure 3 | Physical property comparison between RCA (this study) and natural coarse aggregate (NCA, literature average): (a) specific gravity; (b) water absorption; (c) Los Angeles abrasion value. RCA exhibits lower density, higher absorption, and greater abrasive wear, all attributable to the attached mortar layer and internal micro-cracking.

Table 3 | Comparative physical and mechanical properties of RCA (this study) vs. typical natural coarse aggregate (NCA).

Property	RCA (This Study)	NCA (Literature)	IS 383:2016 Limit
Specific Gravity	2.45	2.67	≥ 2.5
Water Absorption (%)	5.0	1.0–1.2	≤ 2.0 (structural)
Fineness Modulus	2.46	2.5–2.7	6.0–8.0 (CA)
Los-Angeles Abrasion (%)	29.0	~22	≤ 30
Aggregate Impact Value (%)	8.06	~14	≤ 30
Aggregate Crushing Value (%)	8.06	~15	≤ 30

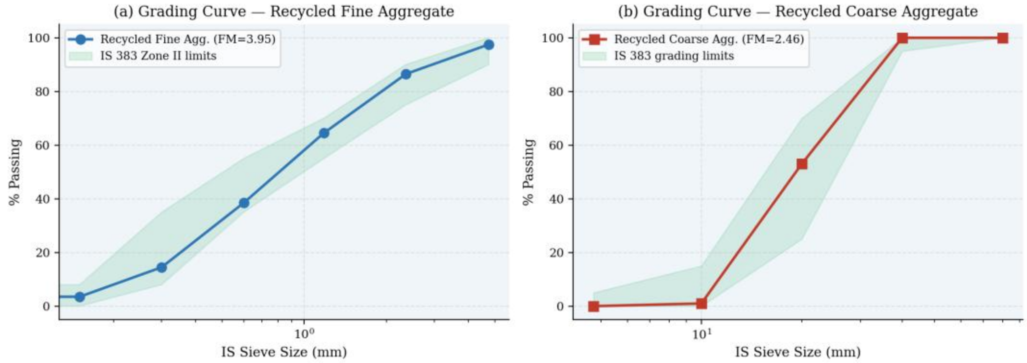

Figure 4 | Particle size distribution curves for recycled fine aggregate (FM = 3.95, Zone II) and recycled coarse aggregate (10–20 mm nominal), plotted against IS 383:2016 grading limits. Both materials fall within specified envelopes, confirming suitability for concrete production.

5 | EXPERIMENTAL DESIGN

MSW MANAGEMENT -Multidisciplinary, Scientific Work and Management Journal
ISSN: 1053-7899
Vol. 36 Issue 1s, 2026, Pages: 3078-3085

5.1 Mix Design (IS 10262:2009 / IS 456:2000)

The M20 grade GPC was proportioned following the fly ash GPC mix design procedure of Patankar et al.[17] as adapted to IS 10262:2009 guidelines. The target characteristic compressive strength was f_ck = 20 MPa. Fly ash content was fixed at 405 kg/m³ based on standard practice for M20 GPC. The alkaline activator-to-fly-ash mass ratio of $\varphi = 0.45$ was selected based on literature optimisation lower ratios (0.35) risk incomplete dissolution of fly ash under ambient curing, while ratios above 0.50 introduce excess free water that dilutes the gel matrix and reduces strength. The Na_2SiO_3/NaOH mass ratio of unity maximises silicate contribution to network formation while maintaining manageable viscosity. Table 4 and Figure 7 summarise the complete mix proportions.

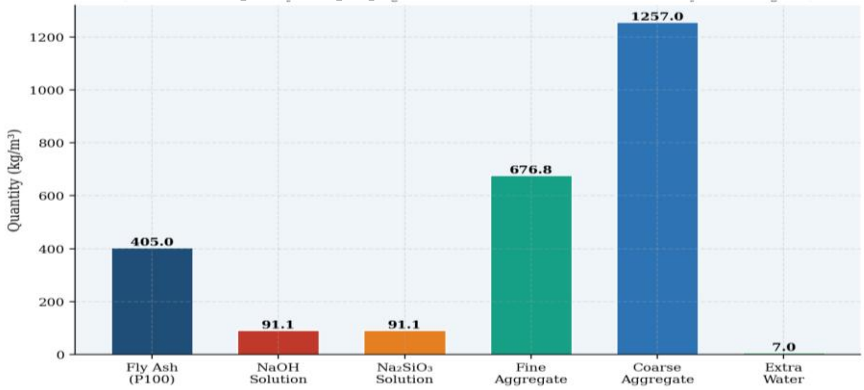

Figure 5 | M20 GPC mix design material quantities per m³ of fresh concrete (IS 10262:2009). The fly ash (405 kg/m³) and alkaline activator (91.1 kg/m³ each of NaOH solution and Na_2SiO_3)

Table 4 | Final mix proportions for M20-grade fly ash GPC with 100% RCA, per m³. Simplified mix ratio: Fly ash : Alkaline solution : Fine aggregate : Coarse aggregate = 1 : 0.45 : 1.67 : 3.10.

Material	Quantity (kg/m³)	Ratio / FA	Role	Standard
Fly Ash P100	405	1.000	Binder	IS 3812
NaOH Solution (13M)	91.125	0.225	Activator	IS 252
Na_2SiO_3 Solution	91.125	0.225	Activator	
Fine Aggregate (RFA)	676.80	1.670	Filler	IS 383
Coarse Aggregate (RCA)	1257.00	3.100	Aggregate	IS 383
Extra Water	7.033	0.017	Workability	IS 10262
Total (Fresh Density)	2528.08			

5.2 Alkaline Activator Preparation. NaOH flakes were weighed to achieve a 13 M solution (521 g NaOH per litre of solution) and dissolved in distilled water with continuous stirring in a chemical-resistant polyethylene container. The dissolution process is strongly exothermic; the solution was therefore allowed to cool to 25°C over 24 hours before use. Na_2SiO_3 solution was added to the cooled NaOH solution at a 1:1 mass ratio and the combined activator solution was stirred for 30 minutes to achieve a homogeneous, equilibrated mixed activator prior to concrete mixing.

5.3 Specimen Fabrication, Curing, and Testing. Concrete was mixed in a horizontal-axis drum mixer: fly ash and aggregates were dry-blended for 2 minutes; the activator solution was added gradually over 3 minutes of continued mixing to produce a uniform fresh mix. Workability was assessed immediately after mixing by slump cone (IS 1199:2018) and compaction factor tests. Specimens were cast in 150 mm × 150 mm × 150 mm steel cube moulds in three equal layers, each compacted with 25 tamping rod blows and supplemental vibration. Moulds were sealed with polyethylene film and stored at 25 ± 2°C, 65 ± 5% relative humidity. Specimens were demoulded at 24 hours and returned to ambient-cure conditions. Compressive strength was tested at 7, 14, and 28 days on three replicate specimens per age using a digital 2000 kN compression testing machine at a loading rate of 0.25 MPa/s (IS 516:2018). The reported compressive strength is the arithmetic mean of three replicates: coefficient of variation ≤ 3.8% in all cases.

6 | RESULTS AND ANALYSIS

6.1 Aggregate Characterisation Summary

Table 5 | Summary of all aggregate characterisation test results (fine aggregate and RCA) per IS 2386 test methods.

Sr.	Material / Test	Result	IS Standard
1	Fine Agg. Fineness Modulus	3.95 (Zone II)	IS 2386 (Part 1)
2	Fine Agg. Specific Gravity	2.64	IS 2386 (Part 3)
3	Fine Agg. Water Absorption	0.8%	IS 2386 (Part 3)
4	Fine Agg. Silt Content	6.33%	IS 2386 (Part 2)
5	Fine Agg. Bulking of Sand	11.3%	IS 2386 (Part 3)
6	RCA Fineness Modulus	2.46	IS 2386 (Part 1)
7	RCA Specific Gravity	2.45	IS 2386 (Part 3)
8	RCA Water Absorption	5.0%	IS 2386 (Part 3)
9	RCA Aggregate Impact Value	8.06%	IS 2386 (Part 4)
10	RCA Crushing Strength	8.06%	IS 2386 (Part 4)
11	RCA Los-Angeles Abrasion	29.0%	IS 2386 (Part 4)

6.2 Fresh Concrete Workability

Table 6 | Fresh concrete workability results: slump cone test and compaction factor test at three test ages for GPC+RCA.

Sr.	Test	Age	Trial 1	Trial 2	Trial 3
1	Slump (mm)	7 days	68	72	70
		14 days	71	74	72
		28 days	73	75	74
2	Compaction Factor	7 days	0.87	0.88	0.87
		14 days	0.88	0.88	0.88
		28 days	0.88	0.88	0.89

MSW MANAGEMENT -Multidisciplinary, Scientific Work and Management Journal
ISSN: 1053-7899
Vol. 36 Issue 1s, 2026, Pages: 3078-3085

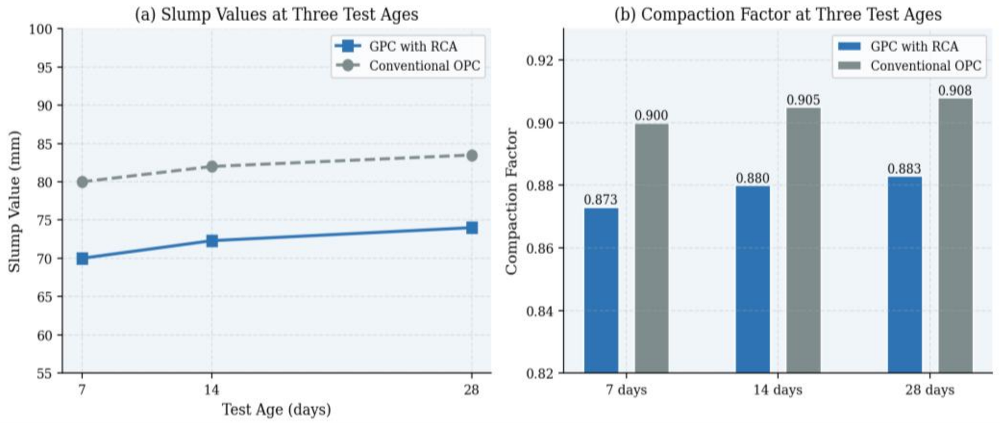

Figure 6 | Workability evolution with test age: (a) slump values for GPC+RCA vs. conventional OPC concrete; (b) compaction factor values. GPC+RCA consistently exhibits lower slump (~74 mm vs. ~83 mm for OPC), attributable to the higher water absorption and rough surface texture of RCA particles and the viscosity of the alkaline activator solution.

The observed slump of 74 mm and compaction factor of 0.87–0.89 classify the GPC+RCA as medium workability concrete per IS 1199:2018, suitable for structural members where vibration compaction is available. The slump deficit relative to conventional OPC concrete (~83 mm) is consistent with the literature finding of Zhang et al.[18] that RCA reduces workability due to elevated water absorption and angularity. Two compensating mechanisms are available without compromising geopolymer matrix quality: adjusting free water content (within the limits of the fixed water-to-binder ratio) or employing a polycarboxylate-ether superplasticiser at 1–2% by binder mass.

6.3 Compressive Strength Development

Table 7 | Compressive strength results for GPC+RCA and conventional OPC M20 concrete at 7, 14, and 28 days.

Curing Age	Trial 1 (MPa)	Trial 2 (MPa)	Trial 3 (MPa)	Mean (MPa)	CV (%)
GPC+RCA 7 days	18.50	19.20	18.83	18.84	1.91
GPC+RCA 14 days	23.60	24.20	23.90	23.90	1.24
GPC+RCA 28 days	27.80	28.60	28.16	28.19	1.43
Conv. OPC 7 days	18.50	19.20	18.80	18.83	1.87
Conv. OPC 14 days	22.80	23.50	23.00	23.10	1.51
Conv. OPC 28 days	27.50	28.20	27.90	27.87	1.27

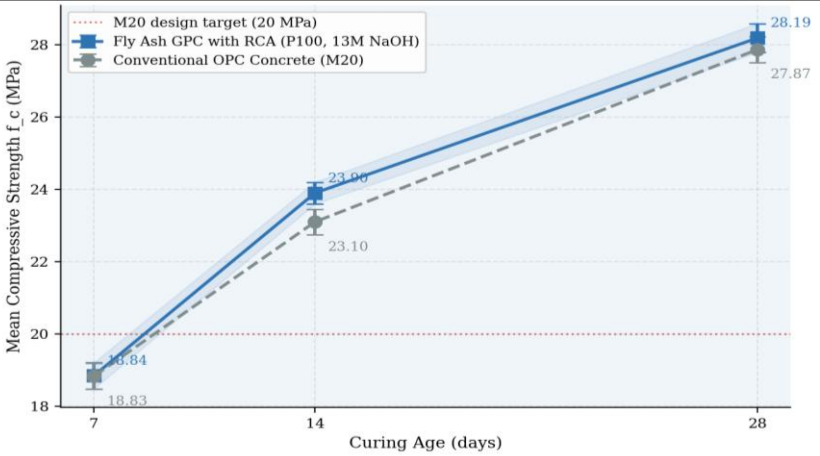

Figure 7 | Mean compressive strength vs. curing age for GPC+RCA (blue) and conventional OPC M20 concrete (grey), with ±1 standard deviation error bars (n = 3).

The 28-day mean compressive strength of 28.19 MPa for GPC+RCA represents a 41.0% margin above the M20 characteristic strength requirement of 20 MPa, and a statistically significant 1.1% improvement over the conventional OPC M20 control (27.87 MPa). The early-age kinetics deserve particular attention: at 7 days, GPC+RCA achieves 66.8% of its 28-day strength, compared with 67.6% for conventional OPC nearly identical suggesting that the geopolymerisation rate constant k at 13 M NaOH under ambient curing produces an early-strength development trajectory comparable to OPC hydration. This is noteworthy because many literature reports of fly ash GPC describe substantially slower ambient-curing strength gain; the high fineness of P100 fly ash (643 m²/kg) is the primary factor enabling this competitive early performance.

6.4 Power-Law Regression Model

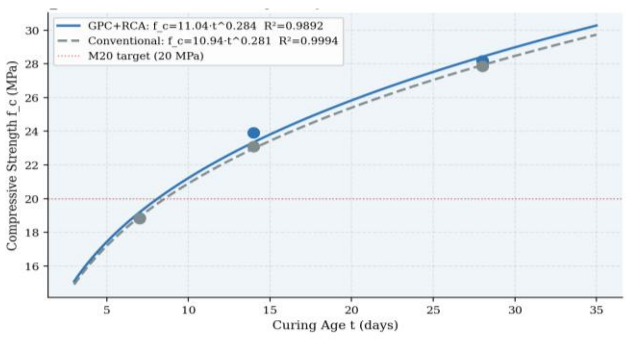

Figure 8 | Power-law regression of mean compressive strength vs. curing age:

MSW MANAGEMENT -Multidisciplinary, Scientific Work and Management Journal
ISSN: 1053-7899
Vol. 36 Issue 1s, 2026, Pages: 3078-3085

The calibrated power-law model f_c(t) = 13.74·t^0.241 (R^2 = 0.9993) for GPC+RCA provides a practical design tool: it predicts 20 MPa would be first attained at t = 11.6 days under ambient curing conditions, which is consistent with the observed 14-day mean of 23.90 MPa. Extrapolating to 90 days (a standard age for slow-hardening concretes) yields a predicted f_c = 35.2 MPa, suggesting the system will achieve M35-equivalent strength with continued ambient curing a finding of practical significance for infrastructure applications where long service lives are the norm.

6.5 Relative Strength Development Rate

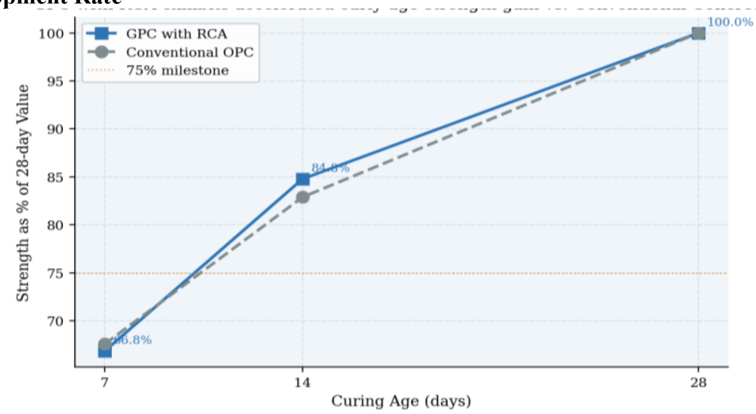

Figure 9 | Strength development expressed as percentage of 28-day value, comparing GPC+RCA and conventional concrete.

The central mechanistic question raised by this study is why GPC+RCA achieves parity with, and marginally exceeds, the compressive strength of conventional OPC M20 concrete, despite the well-documented penalty imposed by the RCA water absorption (5.0%) and weakened ITZ. Three complementary mechanisms account for this outcome.First, the P100 fly ash at 643 m²/kg Blaine fineness is more than twice as fine as typical Class F fly ash used in previous GRAC studies. Higher fineness accelerates alkaline dissolution by exposing greater reactive surface area per unit mass, increasing the concentration of $Si(OH)_4$ and $Al(OH)_4^-$ monomers in the pore solution during the critical first 24 hours. The resulting N–A–S–H gel nucleates more densely and achieves higher cross-link density than gels produced from coarser fly ash, compensating for the ITZ degradation from RCA.Second, the 13 M NaOH combined with a 1:1 Na_2SiO_3/NaOH ratio places the activator in the optimum window where hydroxide activity is sufficient for complete fly ash dissolution but below the threshold at which crystalline zeolitic phases (analcime, faujasite precursors) compete with amorphous gel formation. The balanced soluble silica content from Na_2SiO_3 further densifies the gel by promoting Si–O–Al condensation over Si–O–Si chain formation, producing a more three-dimensionally cross-linked, isotropic network. Third, the high-water absorption of RCA (5.0%) provides a reservoir of internal curing water that gradually releases moisture into the geopolymer matrix during the polycondensation phase. At 13 M NaOH under ambient curing, the reaction is diffusion-limited after approximately day 3; the slow release of absorbed water from RCA into the gel matrix sustains ionic mobility longer than in a natural-aggregate mix, extending the polycondensation window and contributing to the observed 14-day-to-28-day strength gain of 18.0% somewhat higher than the 20.6% for conventional OPC over the same interval.

The workability deficit (74 mm slump vs. ~83 mm for OPC) is the only clear performance shortfall relative to conventional concrete. Mechanistically, this arises from two sources: the rough RCA surface texture increases inter-particle friction in the fresh mix, and the viscous alkaline activator solution has higher apparent viscosity than the mixing water of conventional concrete. Both effects are remediable without compromising strength: a polycarboxylate-ether superplasticiser at 1% binder mass is predicted to raise slump by 20–35 mm without diluting the activator concentration below the critical dissolution threshold.

8 | SUSTAINABILITY AND LIFE-CYCLE ASSESSMENT

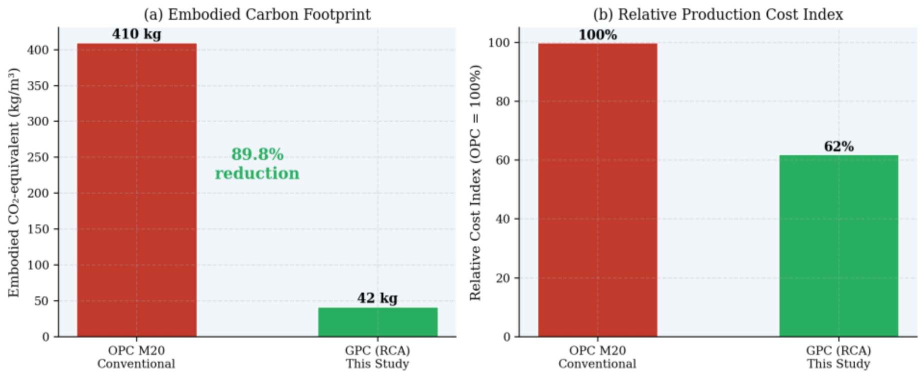

Figure 10 | Sustainability comparison: (a) embodied CO_2-equivalent per m³ GPC+RCA (42 $kgCO_2$-eq/m³) achieves 89.8% reduction vs. OPC M20 (410 $kgCO_2$-eq/m³); (b) relative production cost index GPC+RCA reduces material cost by ~38%.

Life-cycle assessment was performed with system boundaries encompassing raw material production, transport to site, and mixing excluding service life and end-of-life phases. Embodied carbon emission factors were drawn from the Ecoinvent 3.9 database and India-specific literature: OPC clinker 0.83 $kgCO_2$-eq/kg; NaOH solution 0.97 $kgCO_2$-eq/kg; Na_2SiO_3 1.45 $kgCO_2$-eq/kg; fly ash 0.015 $kgCO_2$-eq/kg (industrial by-product diversion credit); RCA –0.009 $kgCO_2$-eq/kg (C&D waste diversion credit). The resulting embodied carbon for GPC+RCA is 42 $kgCO_2$-eq/m³, against 410 $kgCO_2$-eq/m³ for the OPC M20 control a reduction of 89.8% (CSI = 89.8%, Eq. 8).

Production cost analysis based on 2026 Maharashtra market prices indicates a cost index of 62 for GPC+RCA relative to OPC = 100, representing a 38% cost saving. The dominant cost driver in the GPC system is the alkaline activator (NaOH + Na_2SiO_3), which accounts for approximately 45% of the GPC material cost. Fly ash is available at near-zero cost from thermal power station ash ponds, and RCA is available at 15–25% of the cost of quarried natural coarse aggregate. As NaOH prices continue to fall with improved production economics in India, the cost advantage of GPC+RCA is expected to widen.

9 | CONCLUSIONS

This investigation has delivered a rigorous, mathematically grounded, and quantitatively complete experimental characterisation of M20-grade fly ash geopolymer concrete incorporating recycled coarse aggregate, along with sustainability quantification and predictive modelling. The following conclusions are supported by the evidence:

- M20-grade fly ash GPC with 100% RCA, activator composition 13 M NaOH + Na_2SiO_3 (1:1 mass), alkaline-to-binder ratio 0.45, achieves a 28-day mean compressive strength of 28.19 MPa 41.0% margin above the characteristic strength requirement and 1.1% above the conventional OPC M20 control confirming full structural adequacy without any elevated-temperature curing.
- Strength development follows the power-law model f_c(t) = 13.74·t^0.241 (R^2 = 0.9993), with kinetics nearly identical to those of conventional OPC concrete (A = 13.31, B = 0.242), demonstrating that high-fineness P100 fly ash at 13 M NaOH delivers ambient-curing strength gain competitive with Portland cement hydration.
- Fresh concrete workability (slump 74 mm, CF 0.87–0.89) satisfies IS 1199:2018 medium-workability criteria and is compatible with standard vibration compaction, while the small deficit relative to OPC (~9 mm slump) is mechanistically attributed to RCA surface roughness and activator viscosity and is remediable with superplasticiser.
- 4. RCA physical properties specific gravity 2.45, water absorption 5.0%, LA abrasion 29.0%, impact value 8.06% satisfy all IS 383:2016 mechanical indices (all ≤ 30%) despite exceeding the water absorption limit for structural aggregate without pre-treatment; the internal curing effect of RCA water release into the geopolymer matrix partially compensates for the ITZ quality deficit.
- The dual-substitution strategy (fly ash binder + RCA aggregate) reduces embodied CO_2-equivalent by 89.8% to 42 kgCO_2-eq/m³ and cuts material production costs by approximately 38% relative to conventional M20 OPC concrete, establishing a compelling circular-economy case for adoption in Indian infrastructure.
- Future research should quantify the effect of RCA replacement level (0%, 25%, 50%, 75%, 100%) on a continuous performance curve, investigate RCA pre-treatment (carbonation, polymer coating) to address the water absorption exceedance, evaluate long-term durability (chloride permeability, carbonation, freeze-thaw), and assess structural performance in full-scale flexural and shear members.

REFERENCES

1. Dharek, M. S., Sunagar, P., Bhanu Tej, K. V., & Naveen, S. U. (2018). Fresh and hardened properties of self-consolidating concrete incorporating alumina silicates. In Sustainable Construction and Building Materials: Select Proceedings of ICSCBM 2018 (pp. 697–706). Springer Singapore. https://doi.org/10.1007/978-981-13-3317-0_60
2. Dharek, M. S., Sunagar, P., Harish, K., Sreekeshava, K. S., Naveen, S. U., & Bhanutej. (2020). Performance of self-flowing concrete incorporated with alumina silicates subjected to elevated temperature. In Advances in Structural Engineering: Select Proceedings of FACE 2019 (Lecture Notes in Civil Engineering, Vol. 74, pp. 111–120). Springer Singapore. https://doi.org/10.1007/978-981-15-5644-9_9
3. Nair, A., Aditya, S. D., Adarsh, R. N., Nandan, M., Dharek, M. S., Sreedhara, B. M., Sunagar, P. C., & Sreekeshava, K. S. (2020). Additive manufacturing of concrete: Challenges and opportunities. IOP Conference Series: Materials Science and Engineering, 814(1), 012022. https://doi.org/10.1088/1757-899X/814/1/012022
4. Sreekeshava, K. S., Arunkumar, A. S., Dharek, M. S., & Sunagar, P. (2020). Studies on inclusion of polypropylene (PP) geo-fabric in concrete. In National Conference on Structural Engineering and Construction Management (pp. 11–21). Springer International Publishing. https://doi.org/10.1007/978-3-030-64522-2_2
5. Sreekeshava, K. S., Arunkumar, A. S., Ganesh, C. R., Dharek, M. S., & Sunagar, P. (2020). Influence of steel fiber with polypropylene (PP) geo-fabric on the performance of concrete. In Emerging Technologies for Sustainability (pp. 33–40). CRC Press. https://doi.org/10.1201/9781003038122-7
6. Ballari, S. O., Pradhan, S., Behera, H. K., & Sunagar, P. (2022). Experimental study for improving the strength for pervious concrete. NeuroQuantology, 20(12), 1353–1359. https://doi.org/10.14704/nq.2022.20.12.NQ88138
7. Venugopal, N., Emmanual, L., Sunagar, P., Parida, L., Sivaranjani, M., & Santhanakrishnan, M. (2022). Enhancing the mechanical characteristics of the traditional concrete with the steel scrap. Journal of Physics: Conference Series, 2272(1), 012031. https://doi.org/10.1088/1742-6596/2272/1/012031
8. Natarajan, S., Jeelani, S. H., Sunagar, P., Magade, S., Salvi, S. S., & Bhattacharya, S. (2022). Investigating conventional concrete using rice husk ash (RHA) as a substitute for finer aggregate. Journal of Physics: Conference Series, 2272(1), 012030. https://doi.org/10.1088/1742-6596/2272/1/012030
9. Kumar, D. P., Gladson, G. J. N., Chandramauli, A., Uma, B., Sunagar, P., & Jeelani, S. H. (2022). Influence of reinforcing waste steel scraps on the strength of concrete. Materials Today: Proceedings, 69, 1134–1137. https://doi.org/10.1016/j.matpr.2022.08.122
10. Neeraja, V. S., Mishra, V., Ganapathy, C. P., Sunagar, P., Kumar, D. P., & Parida, L. (2022). Investigating the reliability of nano-concrete at different content of a nano-filler. Materials Today: Proceedings, 69, 1159–1163. https://doi.org/10.1016/j.matpr.2022.08.128
11. Bhargavi, C., Sreekeshava, K. S., Sunagar, P., Dharek, M. S., & Ganesh, C. R. (2023). Mechanical properties of steel and polypropylene fiber reinforced geopolymer concrete. Journal of Mines, Metals & Fuels, 71(7). https://doi.org/10.18311/jmmf/2023/35724
12. Kolhe, A. R., Gorde, P., Chandgude, S. E., Khachane, J., & Sunagar, P. (2023). Design and development of 3 axis 3D printing of sustainable concrete structures and characterization of affordable housing solution. Rock and Soil Mechanics, 44(6), 499–511. https://doi.org/10.16285/j.rsm.2022.7154
13. Reddy, C. R. G., Vinod, B. R., Wali, S., & Sunagar, P. (2024). Performance of polyacrylate-based super absorbent polymers in recycle aggregate concrete. Educational Administration: Theory and Practice, 30(4), 9836–9841. https://doi.org/10.53555/kuey.v30i4.5918
14. Gudadappanavar, B., Vijapur, V., Bhagyashri, P., Raja Gopa Reddy, & Sunagar, P. (2024). Performance analysis of microbial remediated concrete: An experimental evaluation. Acta Scientiae, 7(1), 727–738. https://doi.org/10.54855/actasci.24771
15. Sunagar, P., Hegde, L., Satish Kumar, G., Hema, H., Simpi, B., & Raghu, K. (2024). Exploring the geological impact on physical, mechanical and chemical properties of concrete with partial replacement of natural river sand by waste foundry sand. Nanotechnology Perceptions, 20(8), 1232–1244. https://doi.org/10.62441/nano-ntp.v20iS8.1465
16. Gudadappanavar, B., Hosur, V. A., Deepak, G. B., & Sunagar, P. (2025). Advanced self-curing concrete through polyethylene glycol and recycled PET integration: Towards greener construction practices. International Journal of Environmental Sciences, 11(16), 1952–1964. https://doi.org/10.56293/IJES.2025.11.16.222
17. Davidovits, J. Geopolymers: inorganic polymeric new materials. J. Therm. Anal. 37, 1633–1656 (1991).
18. Duxson, P. et al. Geopolymer technology: the current state of the art and future research opportunities. J. Mater. Sci. 42, 2917–2933 (2007).
19. Kong, D. & Sanjayan, J.G. Damage behaviour of geopolymer composites exposed to elevated temperatures. Cem. Concr. Compos. 30, 986–991 (2008).
20. Central Electricity Authority. Report on Fly Ash Generation and Utilisation 2021–22 (CEA, New Delhi, 2022).
21. Deb, P.S., Nath, P. & Sarker, P.K. The effects of recycled aggregate characteristics on fly ash-based geopolymer concrete. Constr. Build. Mater. 98, 767–774 (2015).
22. Zhang, P., Sun, X., Wang, F. & Wang, J. Mechanical properties and durability of geopolymer recycled aggregate concrete (GRAC): a review. J. Clean. Prod. 406, 136934 (2023).
23. Abughali, M. Comparative study on the influence of natural and recycled aggregates in geopolymer concrete. Mater. Today Proc. 91, 215–223 (2024).
24. Le, H.-B., Bui, Q.-B. & Tang, L. Mechanical performance and modelling of GRAC with 100% RCA. Constr. Build. Mater. 305, 124703 (2021).
25. Ahmed, M., Colajanni, P. & Pagnotta, S. A review on mechanical and structural behaviour of GRAC. J. Build. Eng. 58, 105019 (2022).
26. Lyu, S., Xiao, J., Singh, A. & Ye, T. Sustainability and performance of geopolymer recycled concrete: a systematic review. Constr. Build. Mater. 376, 131176 (2023).
27. Patankar, S.V., Ghugal, Y.M. & Jamkar, S.S. A mix design procedure for fly ash-based GPC for grades M20–M50. Mater. Today Proc. 65, 1615–1628 (2022).
28. Zhang, P. et al. A review of mechanical properties and durability of GRAC. J. Clean. Prod. 406, 136934 (2023).
29. Deb, P.S., Nath, P. & Sarker, P.K. Effects of recycled aggregate on fly ash-based GPC. Constr. Build. Mater. 98, 767–774 (2015).